JOURNAL OF SPACECRAFT AND ROCKETS
Vol. 36, No. 6, November–December 1999

Limit Cycle and Chaotic Behavior in Persistent Resonance of Unguided Missiles

Ömer Tanrkulu *
TÜBİTAK-SAGE, 06261 Ankara, Turkey

Flight dynamics problems that are related to the coupling of yaw, pitch, and roll degrees of freedom of unguided missiles have been the subject of a large number of investigations. Special emphasis has been given to persistent resonance and catastrophic yaw phenomena that are caused by nonlinear induced aerodynamic moments and slight configurational asymmetries. Recently, a rigorous analysis of the persistent resonance problem was performed by using a fifth-order autonomous dynamic system model with linear transverse and nonlinear roll aerodynamics. A simple graphical method was used to locate equilibrium points. Stability of equilibrium points were determined by standard linearization. In this study in addition to equilibrium behavior that was examined by previous investigators, the same dynamic system model was found to exhibit limit cycle (periodic) and chaotic (aperiodic) behavior at steady state. Such behavior was examined by using frequency spectra, Poincaré maps, and Lyapunov exponents.

Nomenclature

c = $\sqrt{[-M/(1-\sigma)]}$
G = nonlinear roll aerodynamics coefficient
$\hat{H}$ = transverse damping moment coefficient
h = $(\hat{H} - \sigma\hat{T})/(1-\sigma)$
i = unit imaginary number
$\boldsymbol{J}$ = Jacobian matrix
$\hat{K}_p$ = roll damping coefficient
M = static moment coefficient
p = roll rate, rad/s
p_{res} = linear yaw, pitch, roll resonance roll rate, rad/s
p_s = design roll rate, rad/s
s = $\frac{1}{\lambda}\int_{t_0}^{t} v_C \, \mathrm{d}t$, nondimensional arc-length variable
$\hat{T}$ = Magnus moment coefficient
t = time, s
v_C = speed of center of mass
$\bar{\alpha}$ = scaled angle of attack
$\bar{\beta}$ = scaled angle of side slip
δ_{T_R} = magnitude of trim ξ at linear yaw, pitch, roll resonance, rad
ζ = $\xi/\delta_{T_R} = \bar{\beta} + i\bar{\alpha}$, scaled complex total angle of attack
λ = reference length, m
λ_j = Lyapunov exponent
ξ = $\beta + i\alpha$, complex total angle of attack
σ = ratio of axial moment of inertia to transverse moment of inertia
υ = cs, nondimensional arc-length variable
χ = Euler roll angle, rad
χ_M = slight asymmetry moment orientation angle, rad
χ_s = nondimensional design Euler roll angle rate

Introduction

ONE of the important outcomes of a linear flight dynamics analysis of symmetric unguided missiles was the discovery of yaw-pitch-roll resonance caused by slight configurational asymmetries[1]: If the roll rate p stays sufficiently close to its linear resonance roll rate p_{res} for some time period during flight, then a resonance takes place and magnitude of total complex angle of attack ξ builds up. Despite the fact that unguided missiles are lightly damped systems, probability of a destructive linear resonance seems to be low at a first glance because in general both p and p_{res} change continuously during flight. On the other hand, practical experiences have shown that an unguided missile can fail catastrophically if p is allowed to match p_{res} even for a brief time period.

Significant differences between the results of linear time-invariant theory and experiments led flight dynamicists to focus their attention to nonlinear aerodynamic effects. The discovery was soon made that the highly nonlinear induced roll moment can cause lock-in of p to p_{res} for certain conditions after a linear resonance causes the magnitude of ξ to build up. This type of behavior, which is known as persistent resonance, was later on associated with the much larger roll moment caused by lateral offset of center of mass C from geometrical center O of missile cross section (Fig. 1). Another important discovery was that an unguided missile that is in persistent resonance can become severely unstable for certain conditions because of the highly nonlinear induced yaw and pitch moments. This type of behavior is known as catastrophic yaw. Many researchers have investigated persistent resonance and catastrophic yaw characteristics of free fall bombs, sounding rockets, and reentry vehicles by using a large variety of mathematical models and methods.[2–21]

Persistent resonance followed by catastrophic yaw is one of the most difficult problems to analyze in flight dynamics of unguided missiles, not only because of the strongly nonlinear nature of the problem, but also because of the coupling between yaw, pitch, and roll degrees of freedom. A significant contribution to research in this area was made by Murphy[20] who developed a fifth-order autonomous nonlinear dynamic system model of persistent resonance. Murphy used a linear model for transverse aerodynamics, which included restoring, damping, Magnus, and slight configurational asymmetry moments. He used a nonlinear model for roll aerodynamics, which included linear driving and damping moments, as well as nonlinear roll orientation dependent-induced moment caused by center-of-mass offset. Murphy developed a simple graphical method to determine equilibrium points of his dynamic system model, and he used Lyapunov's linearization method to determine their stability. He determined that three types of equilibrium behavior are possible: design roll $p \approx p_s$, normal persistent resonance roll $p \approx p_{\text{res}}$, and reverse persistent resonance roll $p \approx -p_{\text{res}}$.

Later Ananthkrishnan and Raisinghani[21] examined and corrected a simple mathematical derivation mistake of Murphy. This error is insignificant in terms of location of equilibrium points, but it can be significant in terms of their stability. Some of the case studies of Murphy were performed with the revised model. These same researchers then focused on developing qualitative topological models of the normal and the reverse persistent resonances and concluded that the reverse case is much less likely compared

Presented as Paper 97-3491 at the AIAA Atmospheric Flight Mechanics Conference, New Orleans, LA, 11–13 August 1997; received 22 February 1999; revision received 21 June 1999; accepted for publication 25 June 1999. Copyright © 1999 by the American Institute of Aeronautics and Astronautics, Inc. All rights reserved.

*Coordinator, Mechanics and Systems Engineering Research Group, PK 16, Mamak. Member AIAA.

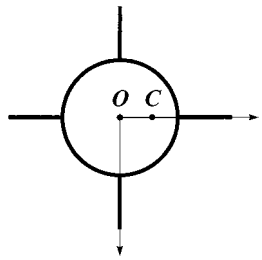

Fig. 1 Offset of center of mass *C* from geometrical center *O*.

to the normal case. Ananthkrishnan and Raisinghani[21] found out through root locus analysis that quasi-steady-state solutions are possible in which unstable ξ oscillations are observed even though p_s is achieved by the missile. (The normal persistent resonance-roll equilibrium point is stable, and the design-roll equilibrium point is unstable.) They tried to construct a topological model of this type of behavior as well and mentioned the possibility of the existence of limit cycles (periodic behavior). Finally, Ananthkrishnan and Raisinghani[21] investigated the problem of catastrophic yaw qualitatively without adding any induced transverse moments into their model. They explained the phenomenon as a case where the normal persistent resonance-roll equilibrium point is unstable because of decreased damping and the design-roll equilibrium point is stable.

A nonlinear system can have four different types of steady-state behavior[22]: equilibrium, periodic, quasiperiodic, and aperiodic. Previous research on yaw, pitch, roll coupling of unguided missiles was focused to equilibrium behavior only. Interestingly enough, both periodic and aperiodic behavior were observed experimentally by Nicolaides[3] during dynamic supersonic wind-tunnel tests of the Aerobee sounding rocket in 1966. In his report[3] Nicolaides made the following comment about the observed aperiodic behavior: "... the missile is seeking three different roll trim angles, 90 deg apart. This 'hunting' characteristic may be due to poor wind tunnel flow or it may be real. Some of our studies suggest that it is real and it is due to poor roll dynamic stability and to serious non-linearities." Since this experimental study of Nicolaides, quasiperiodic and aperiodic oscillation phenomena in yaw, pitch, roll coupling of unguided missiles have remained as untouched problems.

The author has carried out extensive numerical simulations of the analytical persistent resonance model of Murphy as revised by Ananthkrishnan and Raisinghani.[21] This study has revealed the fact that periodic and aperiodic oscillations can be observed in certain cases. In this paper the fifth-order autonomous nonlinear dynamic system model of persistent resonance will be discussed briefly as a first step. Second, several case studies will be presented where equilibrium, periodic and aperiodic behavior are observed at steady state depending on parameters of the model and initial conditions.

Dynamic System Model

Equations of motion of a slightly asymmetric unguided missile with linear transverse aerodynamics and nonlinear roll aerodynamics caused by lateral center of mass offset are presented here[21]:

$$\ddot{\zeta} + [\hat{H} + i(2-\sigma)\dot{\chi}]\dot{\zeta} + [(1-\sigma)(1 + ih\dot{\chi} - \dot{\chi}^2) + i\ddot{\chi}]\zeta = -(1-\sigma)he^{i\chi_M} \tag{1}$$

$$\ddot{\chi} + \hat{K}_p[\dot{\chi} - \dot{\chi}_s + 2G\bar{\alpha}] = 0 \tag{2}$$

Equation (1) is the complex transverse equation of motion, whereas Eq. (2) is the real axial rotational equation of motion. ($\dot{}$) denotes the derivative with respect to the independent variable υ. Equations (1) and (2) were derived in such a way that $\dot{\chi} = 1$ when $p = p_{\text{res}}$. Equations (1) and (2) can also be expressed in state-space form:

$$\dot{\boldsymbol{x}} = \boldsymbol{f}(\boldsymbol{x}), \qquad \boldsymbol{x} \in R^5, \qquad \boldsymbol{f}: R^5 \to R^5 \tag{3}$$

where components of the state vector $\boldsymbol{x}\,(x_j, j = 1, \ldots, 5)$ denote $\dot{\chi}$, $\bar{\beta}$, $\bar{\alpha}$, $\dot{\bar{\beta}}$, and $\dot{\bar{\alpha}}$, respectively. Equation (5) corresponds to five first-order coupled nonlinear differential equations:

$$\dot{x}_1 = -\hat{K}_p x_1 - 2\hat{K}_p G x_3 + \hat{K}_p \dot{\chi}_s \tag{4}$$

$$\dot{x}_2 = x_4 \tag{5}$$

$$\dot{x}_3 = x_5 \tag{6}$$

$$\dot{x}_4 = -\hat{H}x_4 + (2-\sigma)x_1x_5 - (1-\sigma)\left(1 - x_1^2\right)x_2 + [(1-\sigma)h - \hat{K}_p]x_1x_3 + \hat{K}_p x_3(\dot{\chi}_s - 2Gx_3) - (1-\sigma)h\cos\chi_M \tag{7}$$

$$\dot{x}_5 = -\hat{H}x_5 - (2-\sigma)x_1x_4 - (1-\sigma)\left(1 - x_1^2\right)x_3 - [(1-\sigma)h - \hat{K}_p]x_1x_2 + \hat{K}_p x_2(2Gx_3 - \dot{\chi}_s) - (1-\sigma)h\sin\chi_M \tag{8}$$

Equilibrium Behavior

Murphy[20] (and later Ananthkrishnan and Raisinghani[21]) focused on determining location and stability of equilibrium points, where

$$\dot{\boldsymbol{x}} = \boldsymbol{f}(\boldsymbol{x}_{\text{eq}}) = 0 \tag{9}$$

Equation (9) is a set of nonlinear algebraic equations in terms of $\boldsymbol{x}_{\text{eq}}$ and can be solved iteratively by using the Newton–Raphson method. Murphy proposed a simpler graphical method to determine locations of equilibrium points. Equations (1) and (2) simplify as follows at equilibrium:

$$\left(1 + ih\dot{\chi}_{\text{eq}} - \dot{\chi}_{\text{eq}}^2\right)\zeta_{\text{eq}} = -he^{i\chi_M} \tag{10}$$

$$\dot{\chi}_{\text{eq}} - \dot{\chi}_s + 2G\bar{\alpha}_{\text{eq}} = 0 \tag{11}$$

Locations of equilibrium points can be easily found by plotting the functions $f_1(\dot{\chi}) = 2G\bar{\alpha}$ and $f_2(\dot{\chi}) = \dot{\chi} - \dot{\chi}_s$ and by determining their intersections. Stability of the system around a given equilibrium point $\boldsymbol{x}_{\text{eq}}$ can be investigated by examining the time evolution of a small perturbation $\delta\boldsymbol{x}$ from $\boldsymbol{x}_{\text{eq}}$ (Lyapunov's linearization method):

$$\boldsymbol{x} = \boldsymbol{x}_{\text{eq}} + \delta\boldsymbol{x} \tag{12}$$

$$\dot{\boldsymbol{x}}_{\text{eq}} + \delta\dot{\boldsymbol{x}} = \boldsymbol{f}(\boldsymbol{x}_{\text{eq}} + \delta\boldsymbol{x}) = \boldsymbol{f}(\boldsymbol{x}_{\text{eq}}) + \boldsymbol{J}(\boldsymbol{x}_{\text{eq}})\delta\boldsymbol{x} + \text{HOT} \tag{13}$$

$$\delta\dot{\boldsymbol{x}} \approx \boldsymbol{J}(\boldsymbol{x}_{\text{eq}})\delta\boldsymbol{x} \tag{14}$$

Hence, stability of $\boldsymbol{x}_{\text{eq}}$ can simply be determined by calculating eigenvalues of the Jacobian matrix $\boldsymbol{J}$ at $\boldsymbol{x}_{\text{eq}}$. $\dot{\chi}_s$, G, χ_M, and h influence the location of equilibrium points, whereas $\dot{\chi}_s$, G, χ_M, h, $\hat{H}$, $\hat{K}_p$, and σ all affect their stability.

Murphy[20] and later on Ananthkrishnan and Raisinghani[21] performed numerical case studies to examine dynamics of the persistent resonance model. System parameter values that they used in one of their case studies are as follows: $h = \hat{H} = \hat{K}_p = \sigma = 0.1$, $\dot{\chi}_s = 3.0$, and $G = 5.0$. Figure 2 shows location of possible equilibrium points

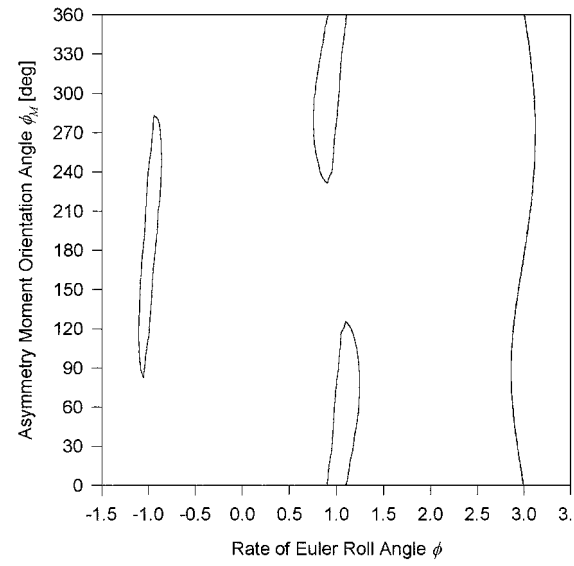

Fig. 2 Location of possible equilibrium points for $\dot{\phi}_s$ = 3.0.

that were determined by finding intersections of the functions $f_1(\dot{\chi})$ and $f_2(\dot{\chi})$ with the given parameter values. There are five possible equilibrium points when $\chi_M = 90$ deg. Ananthkrishnan and Raisinghani[21] carried out linear stability analysis and found out that only two of these equilibrium points are stable: A normal persistent resonance equilibrium point with $\dot{\chi}_{eq} = 1.011$ and a design roll equilibrium point with $\dot{\chi}_{eq} = 2.861$. In another case study Murphy[20] and later on Ananthkrishnan and Raisinghani[21] used the following system parameter values: $h = \hat{H} = \hat{K}_p = \sigma = 0.1$, $\dot{\chi}_s = 3.0$, $G = 5.0$, and $\chi_M = 270$ deg. (In all of the case studies to be discussed in this paper, $h = \hat{H} = \hat{K}_p = \sigma = 0.1$ and $G = 5.0$. Different cases will be specified by their $\dot{\chi}_s$ and χ_M values.) Similar to the first case with $\chi_M = 90$ deg just discussed, there are five possible equilibrium points for this case (Fig. 2), and only two of these are stable: a reverse persistent resonance equilibrium point with $\dot{\chi}_{eq} = -0.976$ and a design roll equilibrium point with $\dot{\chi}_{eq} = 3.115$. Stability results of Murphy[20] were qualitatively the same as those of Ananthkrishnan and Raisinghani[21] for the first and the second cases despite Murphy's derivation mistake. Reference 21 gives eigenvalues of the Jacobian matrix $\boldsymbol{J}$ both at stable and unstable equilibrium points for both of the cases. Different initial conditions can lead to different types of dynamic behavior. In Figs. 3 and 4 responses of the system ($\dot{\chi}_s = 3.0$, $\chi_M = 90$ deg) to the following four basic initial conditions are shown: $\boldsymbol{x}(0)_1^T = \{0, 0, 0, 1, 0\}$, $\boldsymbol{x}(0)_2^T = \{0, 0, 0, 0, 1\}$, $\boldsymbol{x}(0)_3^T = \{0, 0, 0, -1, 0\}$, and $\boldsymbol{x}(0)_4^T = \{0, 0, 0, 0, -1\}$. (Superscript T indicates vector transpose operation.) $\boldsymbol{x}(0)_1$ and $\boldsymbol{x}(0)_2$ lead to the design-roll equilibrium point ($\dot{\chi}_{eq} = 2.861$), whereas $\boldsymbol{x}(0)_3$ and $\boldsymbol{x}(0)_4$ lead to the normal persistent resonance equilibrium point ($\dot{\chi}_{eq} = 1.011$). (The numerical simulations that are presented in this paper were performed with the INSITE software,[22] which uses a fourth-order Runge–Kutta integration routine. The step size is $\Delta\upsilon = 0.1$ in all simulations.)

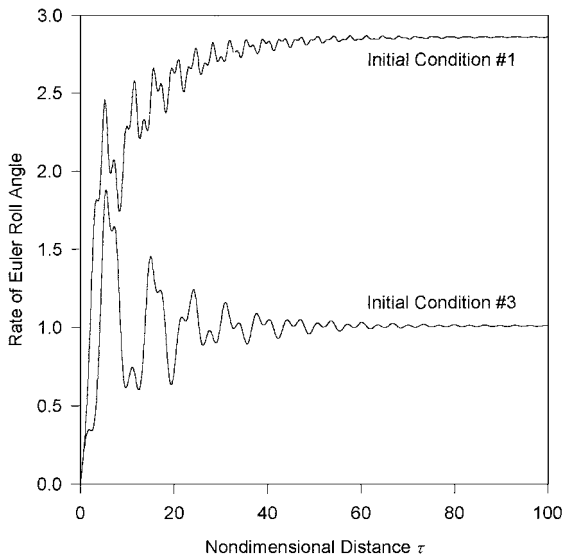

Fig. 3 $\dot{\phi}_s$ vs τ for $\boldsymbol{x}(0)_1$ and $\boldsymbol{x}(0)_3$ ($\dot{\phi}_s = 3.0$, $\phi_M = 90$ deg).

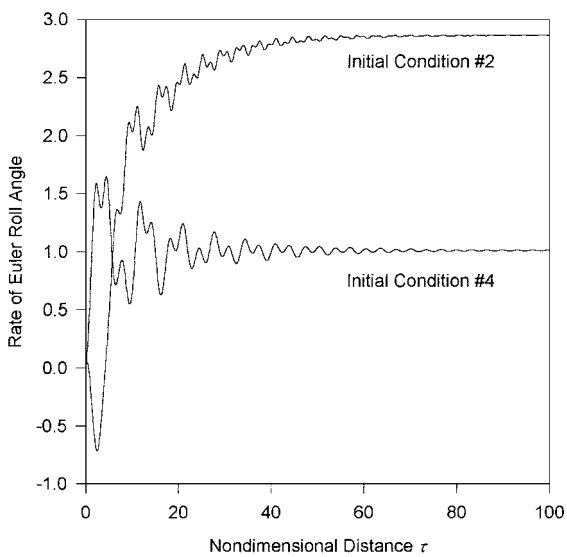

Fig. 4 $\dot{\phi}_s$ vs τ for $\boldsymbol{x}(0)_2$ and $\boldsymbol{x}(0)_4$ ($\dot{\phi}_s = 3.0$, $\phi_M = 90$ deg).

Periodic Behavior

A set of numerical experiments was performed in which effect of χ_M on response of the dynamic system model was examined systematically. The value of χ_M was increased with 10-deg increments in the 0–360-deg interval while the value of $\dot{\chi}_s$ was kept constant as 3.0. At each χ_M value steady-state responses to the four basic initial conditions were determined. Results of these numerical experiments are presented in Fig. 5, where regions of χ_M that lead to

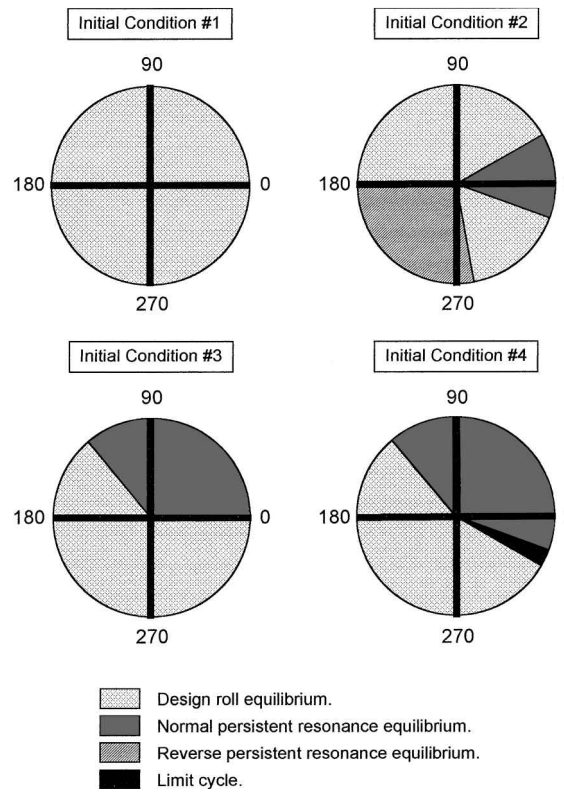

Fig. 5 Effect of ϕ_M on response for $\dot{\phi}_s = 3.0$.

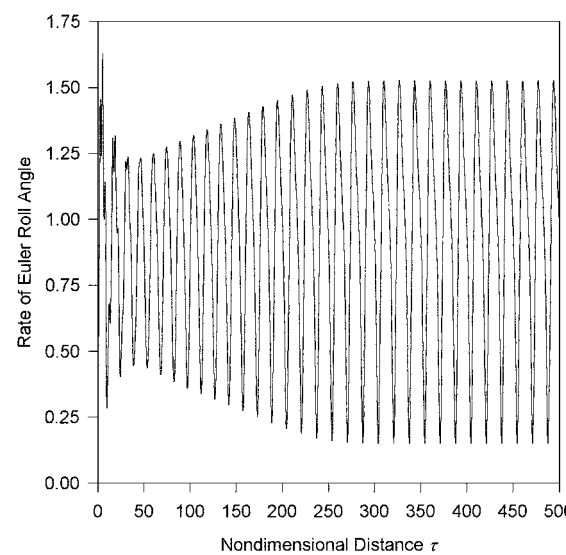

Fig. 6 Variation of $\dot{\phi}$ with τ for $\boldsymbol{x}(0)_4$ and ($\dot{\phi}_s = 3.0$, $\phi_M = 330$ deg).

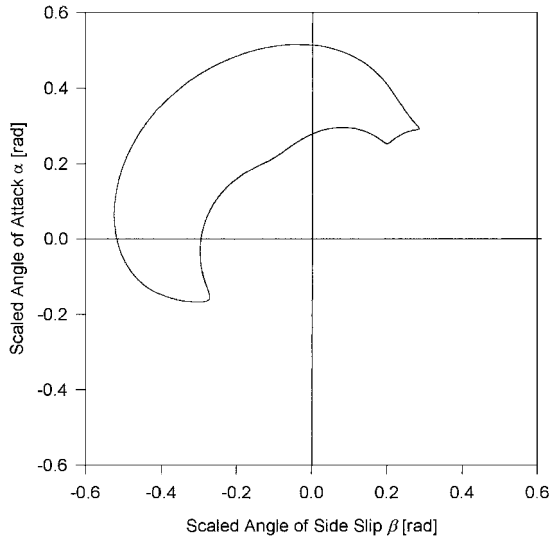

Fig. 7 Variation of $\bar{\beta}$ with $\bar{\alpha}$ for $x(0)_4$ and ($\dot{\phi}_s$ = 3.0, ϕ_M = 330 deg).

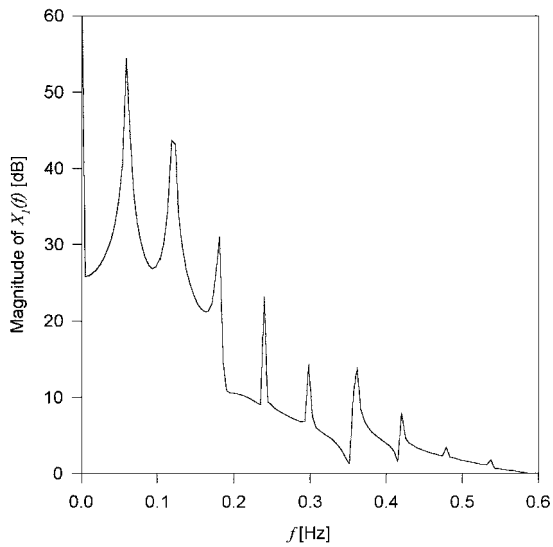

Fig. 8 Spectrum of $\dot{\phi}$ for periodic behavior for ($\dot{\phi}_s$ = 3.0, ϕ_M = 330 deg).

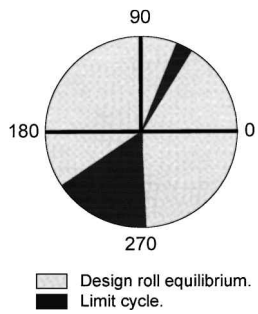

Fig. 9 Effect of orientation of $\dot{\zeta}(0)$ on response for ($\dot{\phi}_s$ = 3.0, ϕ_M = 330 deg).

different types of steady-state behavior are shown for each initial condition by using pie charts. An interesting result was obtained for the fourth initial condition, where a limit cycle (periodic behavior) was obtained for $\chi_M = 330$ deg. Figure 6 shows the variation of $\dot{\chi}$ with υ, and Fig. 7 shows the variation of $\bar{\beta}$ with $\bar{\alpha}$ at steady state for this particular case. Figure 8 shows magnitude of spectrum of $\dot{\chi}$, which clearly indicates periodic nature of oscillations: The fundamental harmonic has a frequency of $f = 0.058$ Hz, and there are superharmonics with frequencies that are integer multiples of the fundamental harmonic. Lyapunov exponents[22] of the limit cycle were determined by using INSITE as follows: $\lambda_1 = 0.0114$, $\lambda_2 = -0.0238$, $\lambda_3 = -0.0450$, $\lambda_4 = -0.0572$, and $\lambda_5 = -0.1860$. Theoretically, one of the Lyapunov exponents of a periodic attractor should be equal to zero, the remaining ones should be negative.[22] INSITE's prediction of $\lambda_1 \approx 0$, $\lambda_2 < 0$, $\lambda_3 < 0$, $\lambda_4 < 0$, and $\lambda_5 < 0$ verifies periodic nature of oscillations for $\chi_M = 330$ deg.

As can be seen from Fig. 5, periodic behavior is observed for a very narrow range of χ_M values. A set of numerical experiments was performed with $\chi_M = 330$ deg and $\dot{\chi}_s = 3.0$. Magnitude of $\dot{\zeta}(0)$ was taken as 1.0, while its orientation angle was increased with 10-deg increments in the 0–360-deg interval. Initial values of the other state variables were taken as zero. Results of these numerical experiments are shown in Fig. 9, where the type of steady-state behavior reached with different $\dot{\zeta}(0)$ are presented in the form of a pie chart. Figure 9 shows that for $\chi_M = 330$ deg a significant proportion of initial conditions do lead to periodic oscillations, whereas the majority of initial conditions result in design-roll equilibrium. (There are three possible equilibrium points when $\chi_M = 330$ deg, as can be seen from Fig. 2. Stability analysis shows that only the design-roll equilibrium with $\dot{\chi}_{eq} = 3.056$ is stable.)

Aperiodic Behavior

A set of numerical experiments was performed in which effect of $\dot{\chi}_s$ on the response of the dynamic system model with $\chi_M = 330$ deg was examined systematically. The value of $\dot{\chi}_s$ was increased with 0.25 increments in the 0.5–3.0 interval, and at each increment response to the first basic initial condition $\boldsymbol{x}(0)_1^T = \{0, 0, 0, 1, 0\}$ was determined. Equilibrium behavior was obtained for all cases except for the case with $\dot{\chi}_s = 1.25$, which exhibited chaotic (aperiodic) oscillations.

Recent research on nonlinear system dynamics has shown that there are universal rules of transition to chaos: period doubling, quasiperiodicity, intermittency, chaotic transients, and crises.[22,23] A new set of numerical experiments was performed to determine the mechanism of transition to chaos that was observed for $\dot{\chi}_s = 1.25$: The value of $\dot{\chi}_s$ was increased with 0.01 increments starting from $\dot{\chi}_s = 1.20$, and at each increment the response to the first basic initial condition $\boldsymbol{x}(0)_1^T = \{0, 0, 0, 1, 0\}$ was determined. Figure 10 shows variation of $\dot{\chi}$ with υ for $\dot{\chi}_s = 1.20$, $\dot{\chi}_s = 1.21$, and $\dot{\chi}_s = 1.22$. The system exhibits nonresonant equilibrium at steady state for $\dot{\chi}_s = 1.20$. When $\dot{\chi}_s$ is increased to 1.21, the system exhibits chaotic (aperiodic) oscillations until $\upsilon \approx 750$, which then damp to nonresonant equilibrium at steady state. When $\dot{\chi}_s$ is further increased to 1.22, the system exhibits chaotic oscillations even at steady state. Figure 11 shows variation of $\bar{\beta}$ with $\bar{\alpha}$ for $\dot{\chi}_s = 1.22$. This type of transition to chaos is known as chaotic transients, and it takes place when stable and unstable manifolds of an equilibrium

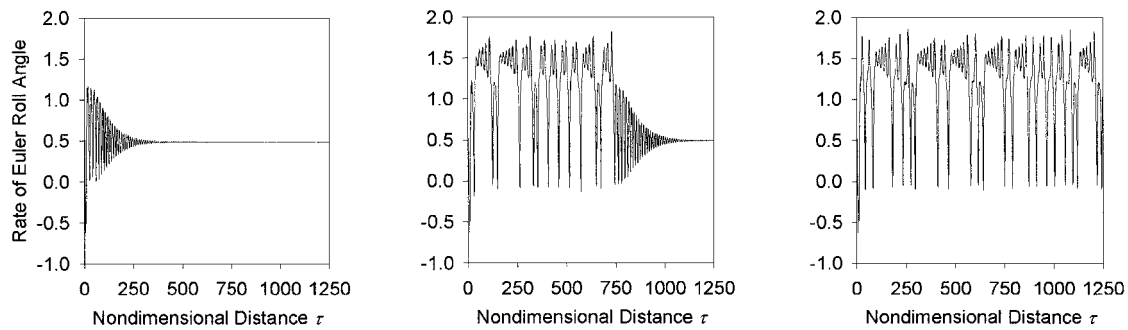

Fig. 10 $\dot{\phi}$ vs τ for $\dot{\phi}_s$ = 1.20, 1.21, 1.22, respectively, for $x(0)_1$ and ϕ_M = 330 deg.

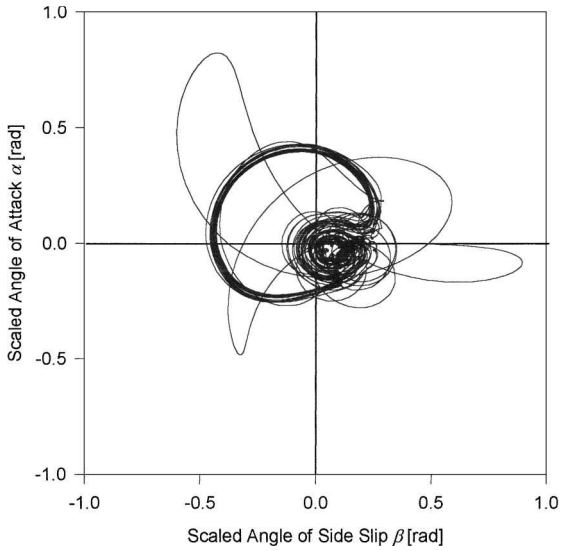

Fig. 11 Variation of $\bar{\beta}$ with $\bar{\alpha}$ for $x(0)_1$ and ($\dot{\phi}_s$ = 1.22, ϕ_M = 330 deg).

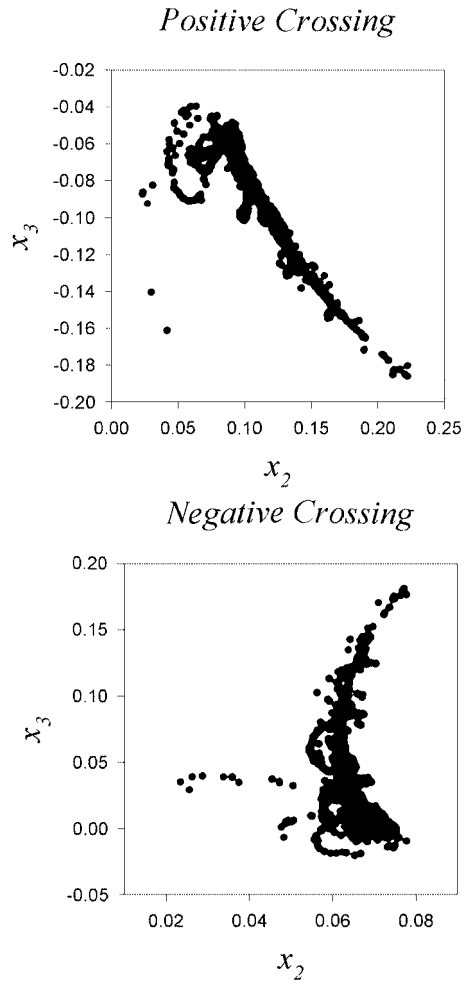

Fig. 12 Poincaré maps of aperiodic behavior for ($\dot{\phi}_s$ = 1.22, ϕ_M = 330 deg).

(or periodic) attractor intersect (homoclinic intersection) or two different equilibrium (or periodic) attractors intersect (heteroclinic intersection) at a certain value of the control parameter.[23] A single homoclinic or heteroclinic intersection indicates infinitely many such intersections and results in homoclinic or heteroclinic tangles. Figure 12 shows positive and negative crossing Poincaré maps of the aperiodic attractor for $\dot{\chi}_s = 1.22$. Poincaré plane is defined as $x_1 = \dot{\chi} = 1.5$. Tangle behavior can be seen in both Poincaré maps. Chaotic transients route to chaos was also observed in other experiments in which G or χ_M was used as the control parameter.

Figure 13 shows magnitude of spectrum of $\dot{\chi}$ for $\dot{\chi}_s = 1.22$ and $\boldsymbol{x}(0)_1^T = \{0, 0, 0, 1, 0\}$; the continuous spectrum indicates chaotic oscillations. Lyapunov exponents of this aperiodic behavior were determined by using INSITE as follows: $\lambda_1 = 0.0337$, $\lambda_2 = 0.0002$, $\lambda_3 = -0.0327$, $\lambda_4 = -0.0648$, and $\lambda_5 = -0.2366$. Theoretically at least one of the Lyapunov exponents of an aperiodic attractor should be positive, one of the remaining should be equal to zero, and the others should be negative.[22] INSITE's prediction of $\lambda_1 > 0$, $\lambda_2 \approx 0$, $\lambda_3 < 0$, $\lambda_4 < 0$, and $\lambda_5 < 0$ verifies the aperiodic nature of oscillations for $\dot{\chi}_s = 1.22$.

Figure 14 shows that there are three possible equilibrium points for ($\dot{\chi}_s = 1.22$, $\chi_M = 330$ deg): two nonresonant equilibrium points with $\dot{\chi}_{eq} = 0.491$ and $\dot{\chi}_{eq} = 1.521$ and one normal persistent resonance equilibrium point with $\dot{\chi}_{eq} = 1.085$. Linear stability analysis showed that only the nonresonant equilibrium point with $\dot{\chi}_{eq} = 0.491$ is stable.

A set of numerical experiments was performed in which the effect of χ_M on responses to the four basic initial conditions was examined systematically ($\chi_M = 0, 10, 20, \ldots, 350$ deg) for $\dot{\chi}_s = 1.22$. Results of these numerical experiments are presented in Fig. 15, which shows that aperiodic behavior takes place for the first initial condition and for a very narrow range of χ_M values. One must also

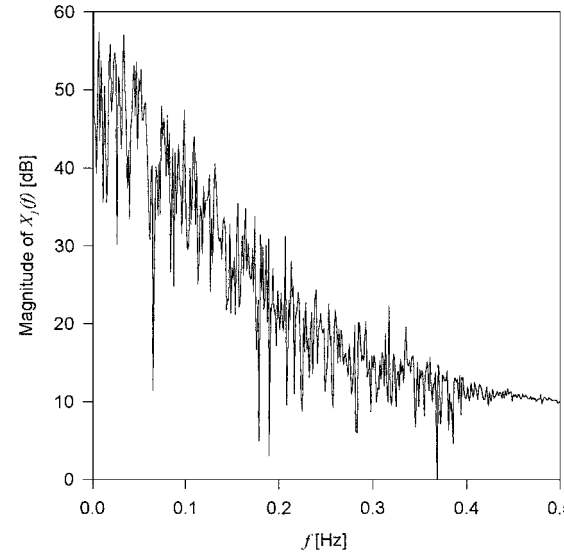

Fig. 13 Spectrum of aperiodic behavior for ($\dot{\phi}_s$ = 1.22, ϕ_M = 330 deg).

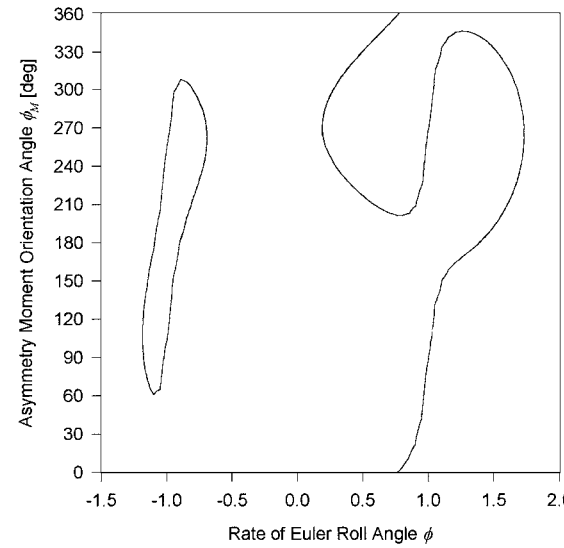

Fig. 14 Location of possible equilibrium points for $\dot{\phi}_s$ = 1.22.

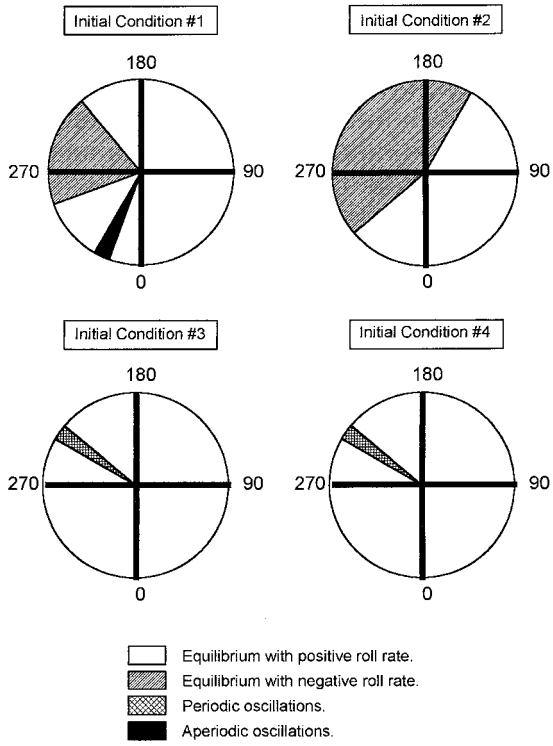

Fig. 15 Effect of ϕ_M on response for $\dot{\phi}_s = 1.22$.

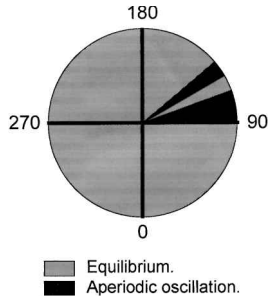

Fig. 16 Effect of orientation of $\dot{\zeta}(0)$ on response for ($\dot{\phi}_s$ = 1.22, ϕ_M = 330 deg).

note that reverse persistent resonance is much more likely when the value of $\dot{\chi}_s$ is reduced from 3.0 to 1.22.

A set of numerical experiment was performed in which the effect of orientation of $\dot{\zeta}(0)$ to response was investigated for $\chi_M = 330$ deg and $\dot{\chi}_s = 1.22$. Magnitude of $\dot{\zeta}(0)$ was taken as 1.0, while its orientation angle was increased with 10-deg increments in the 0–360-deg interval. Initial values of other state variables were taken as zero. Results of these numerical experiments are given in Fig. 16, which shows that almost all of the initial conditions lead to the nonresonant equilibrium point with $\dot{\chi}_{eq} = 0.491$.

Discussion

A survey of the technical literature about flight dynamics of unguided missiles shows that most of the publications are on quasi-linear or perturbation analysis of nonlinear problems. These methods were also widely used by specialists in other branches of science and engineering until the research on chaos created a revolution in nonlinear system dynamics. Interestingly enough, this revolution did not have any significant impact on research on flight dynamics of unguided missiles.

The research of Murphy[20] on persistent resonance is very important because of two reasons: First, he discovered that reverse persistent resonance equilibrium is possible, which is significant in terms of flight dynamics design. Second, he used the state-space formulation to analyze coupled axial and transverse dynamics in nondimensional distance domain by using numerical integration. He did not linearize or quasi-linearize.

This study shows that the persistent resonance model of Murphy can exhibit much more complicated behavior. Periodic and aperiodic attractors that were just examined have significance in terms of engineering design. In the case of the periodic attractor, roll rate oscillates between approximately 0.2 and 1.5 rather than converging to the design-roll equilibrium of 3.0. In the case of the aperiodic attractor, roll rate oscillates erratically between approximately −0.1 and 1.75 rather than converging to the design-roll equilibrium of 1.25. The periodic attractor is also characterized by ξ oscillations with large amplitude. Hence, neither periodic nor aperiodic behavior would be acceptable in terms of flight dynamics design.

Conclusion

In this paper dynamic behavior of a single unguided missile was examined for two different values of cant angle of tail fins ($\dot{\chi}_s$), 36 values of asymmetry moment orientation angle (χ_M), and a small number of initial conditions. Moreover, the present dynamic system model is limited because it does not include any transverse nonlinearities due to cubic restoring, damping, and Magnus moments as well as induced moments. Hence, it should be extremely wrong to classify periodic and aperiodic behavior as rare phenomena in yaw, pitch, roll coupling of unguided missiles based on the case studies that were just presented. The research of Nicolaides[3] on the Aerobee sounding rocket in which periodic and aperiodic oscillations were observed experimentally must be noted.

Nonlinear system dynamicists are experienced in analyzing periodic behavior, by using quasi-linear methods. On the other hand, there are no conventional analysis methods for aperiodic behavior, and therefore it was almost always attributed to numerical instabilities or experimental noise before the major developments in chaos theory took place in the 1980s. Flight dynamicists who specialize in unguided missiles may have made the similar common error of considering aperiodic oscillations as pathological cases.

References

[1]Nicolaides, J. D., "On the Free Flight Motion of Missiles Having Slight Configurational Asymmetries," U.S. Army Ballistic Research Lab., BRL Rept. 858, AD 26405, Aberdeen Proving Ground, MD, June 1952.

[2]Glover, L. S., "Effects on Roll Rate of Mass and Aerodynamic Asymmetries for Ballistic Re-Entry Bodies," *Journal of Spacecraft and Rockets*, Vol. 2, No. 2, 1965, pp. 220–225.

[3]Nicolaides, J. D., "A Review of Some Recent Progress in Understanding Catastrophic Yaw," Rept. 551, AGARD, 1966.

[4]Daniels, P., "Fin-Slots Versus Roll Lock-In and Roll Speed Up," *Journal of Spacecraft and Rockets*, Vol. 4, No. 3, 1967, pp. 410–412.

[5]Chadwick, W. R., "Flight Dynamics of a Bomb with Cruciform Tail," *Journal of Spacecraft and Rockets*, Vol. 4, No. 6, 1967, pp. 768–773.

[6]Platus, D. H., "A Note on Re-Entry Vehicle Roll Resonance," *AIAA Journal*, Vol. 5, No. 7, 1967, pp. 1348–1350.

[7]Price, D. A., Jr., "Sources, Mechanisms, and Control of Roll Resonance Phenomena for Sounding Rockets," *Journal of Spacecraft and Rockets*, Vol. 4, No. 11, 1967, pp. 1516–1525.

[8]Vaughn, H. R., "Boundary Conditions for Persistent Roll Resonance on Re-Entry Vehicles," *AIAA Journal*, Vol. 6, No. 6, 1968, pp. 1030–1035.

[9]Barbera, F. J., "An Analytical Technique for Studying the Anomalous Roll Behavior of Re-Entry Vehicles," *Journal of Spacecraft and Rockets*, Vol. 6, No. 11, 1969, pp. 1279–1284.

[10]Nayfeh, A. H., "A Multiple Time Scaling Analysis of Re-Entry Roll Dynamics," *AIAA Journal*, Vol. 7, No. 11, 1969, pp. 2155–2157.

[11]Daniels, P., "A Study of the Non-Linear Rolling Motion of a Four-Finned Missile," *Journal of Spacecraft and Rockets*, Vol. 7, No. 4, 1970, pp. 510–512.

[12]Price, D. A., Jr., and Ericsson, L. E., "A New Treatment for Roll-Pitch Coupling for Ballistic Re-Entry Vehicles," *AIAA Journal*, Vol. 8, No. 9, 1970, pp. 1608–1615.

[13]Clare, T. A., "Resonance Instability for Finned Configurations Having Non-Linear Aerodynamic Properties," *Journal of Spacecraft and Rockets*, Vol. 8, No. 3, 1971, pp. 278–283.

[14]Bootle, W. J., "Spin Variations in Slender Entry Vehicles During Rolling Trim," *AIAA Journal*, Vol. 9, No. 4, 1971, pp. 729–731.

[15]Madden, R. G., "A Statistical Analysis of the Roll Rate of a Launch Vehicle Under the Influence of Random Fin Misalignments," *AIAA Journal*, Vol. 10, No. 3, 1972, pp. 324, 325.

[16]Nayfeh, A. H., and Saric, W. S., "An Analysis of Asymmetric Rolling Bodies with Non-Linear Aerodynamics," *AIAA Journal*, Vol. 10, No. 8, 1972, pp. 1004–1011.

[17]Cohen, C. J., Clare, T., and Stevens, F. L., "Analysis of the Non-Linear Rolling Motion of Finned Missiles," *AIAA Journal*, Vol. 12, No. 3, 1974, pp. 303–309.

[18]Pepitone, T. R., and Jacobson, I. D., "Resonant Behavior of a Symmetric Missile Having Roll Orientation-Dependent Aerodynamics," *Journal of Guidance and Control*, Vol. 1, No. 5, 1978, pp. 335–339.

[19]Bennett, M. D., "Roll Resonance Probability for Ballistic Missiles with Random Configurational Asymmetry," *Journal of Guidance, Control, and Dynamics*, Vol. 6, No. 3, 1983, pp. 222–224.

[20]Murphy, C. H., "Some Special Cases of Spin-Yaw Lock-In," *Journal of Guidance, Control, and Dynamics*, Vol. 12, No. 6, 1989, pp. 771–776.

[21]Ananthkrishnan, N., and Raisinghani, S. C., "Steady and Quasi-Steady Resonant Lock-In of Finned Projectiles," *Journal of Spacecraft and Rockets*, Vol. 29, No. 5, 1992, pp. 692-696.

[22]Parker, T. S., and Chua, L.O., *Practical Numerical Algorithms for Chaotic Systems*, 1st ed., Springer–Verlag, New York, 1989.

[23]Hilborn, R. C., *Chaos and Non-Linear Dynamics*, 1st ed., Oxford Univ. Press, New York, 1994.

F. H. Lutze Jr.
Associate Editor